Available online at www.sciencedirect.com
ScienceDirect
Journal of the European Ceramic Society 29 (2009) 931–935
www.elsevier.com/locate/jeurceramsoc

Shaping of advanced asymmetric structures of proton conducting ceramic materials for SOFC and membrane-based process applications

M.L. Fontaine [a,*], Y. Larring [a], J.B. Smith [a], H. Raeder [a], Ø.S. Andersen [b], M.-A. Einarsrud [b], K. Wiik [b], R. Bredesen [a]

[a] *SINTEF Materials and Chemistry, PB 124 Blindern, N-0314 Oslo, Norway*
[b] *Department of Materials Science and Engineering, NTNU 7491 Alfred Getzv. 2, Trondheim, Norway*

Available online 6 September 2008

Abstract

A versatile fabrication process combining three techniques easy to scale up was successfully developed to prepare advanced multilayered structures integrating proton conducting ceramic materials. This enables the production of novel solid oxide fuel cells with proton conducting electrolytes (PCFCs) and asymmetric membranes designed as thin dense layers coated on thick porous mechanical supports. The manufacturing process makes use of ceramic powders synthesized by spray-pyrolysis using water-based solutions. Porous supports of membranes and anodes of PCFCs were prepared by tape-casting and their porosity was tuned by addition of corn starch filler. Membrane and electrolyte layers were prepared by spin-coating colloidal ceramic suspensions. A single coating-sintering step was carried out to produce gas tight layers with thickness ranging from 4 to 26 μm. Cathodes of PCFCs were screen-printed using commercial Pt ink. This paper describes the successful preparation of $SrCe_{0.95}Yb_{0.05}O_{3-\delta}$ asymmetric membranes and novel concepts of PCFCs integrating $BaZr_{0.9}Y_{0.1}O_{3-\delta}$ and $La_{0.995}Sr_{0.005}NbO_{4+\delta}$ electrolytes.

Keywords: Ceramic proton conductors; Hydrogen membranes; Fuel cells; Tape-casting; Spin coating

1. Introduction

In solid oxide fuel cell and hydrogen separation technologies, ceramic proton conducting devices have attracted considerable attention. Dense ceramic membranes of mixed proton and electron conductors may provide a simple and efficient way to separate H_2 from a gas stream. The efficiency of these devices strongly depends on the performance of the dense ceramic membranes in which hydrogen transport takes place by diffusion of protons. The diffusion occurs mainly through the bulk and the flux is often inversely dependent on the membrane thickness. It is therefore very desirable to develop thin membranes.

Various attempts have been made to develop time- and cost-effective processes allowing the preparation of thin dense ion conducting ceramic films coated onto porous supports.[1–3] Numerous factors can challenge successful preparation, e.g., chemical reactivity and/or the thermo-mechanical mismatch at the interface between the dense layer and the porous support. Additionally, most of techniques currently used are expensive or difficult to scale-up, such as hydrothermal process, metal-organic chemical vapor deposition (MO-CVD) and atmospheric spray pyrolysis, and time consuming due to the need to repeat cycles of coating and thermal treatment, as often encountered with chemical solution deposition techniques.[4–8] Among other critical issues to address, proton conducting materials generally require high sintering temperature that may result in segregation of dopants, impurities, secondary phases, and pore trapping in grain boundaries. This may lead to undesirable effects like significant increase in resistivity in the functional layers, and subsequently, low performance of the fuel cell or the hydrogen membrane.

To address these bottlenecks, our efforts focused on the production of new materials and architectures starting with the synthesis of powders exhibiting high sinterability. Spray-pyrolysis technique was chosen for this purpose, as it allows reliable batch scale production of powder with controlled morphology and composition. Water-based solutions were used to prepare proton conducting $BaZr_{0.9}Y_{0.1}O_{3-\delta}$ and $La_{0.995}Sr_{0.005}NbO_{4+\delta}$ oxides and mixed proton and electron conducting $SrCe_{0.95}Yb_{0.05}O_{3-\delta}$ oxide. These powders were further used for the preparation of novel multilayered structures by means of a time- and cost-effective processing

* Corresponding author. Tel.: +47 93 47 95 55.
E-mail address: marie-laure.fontaine@sintef.no (M.L. Fontaine).

0955-2219/$ – see front matter © 2008 Elsevier Ltd. All rights reserved.
doi:10.1016/j.jeurceramsoc.2008.07.028

combining tape-casting, spin-coating and screen-printing techniques. $BaZr_{0.9}Y_{0.1}O_{3-\delta}$ perovskite oxide and strontium doped $La_{0.995}Sr_{0.005}NbO_{4+\delta}$ monazite oxide were used for the preparation of fuel cells with respect to their high mechanical stability and appreciable proton conductivity as electrolyte materials.[9,10] $SrCe_{0.95}Yb_{0.05}O_{3-\delta}$ perovskite oxide was used for the preparation of asymmetric membranes.[11]

2. Experimental procedure

2.1. Preparation of dense ceramic films

$BaZr_{0.9}Y_{0.1}O_{3-\delta}$ (BZY), $SrCe_{0.95}Yb_{0.05}O_{3-\delta}$ (SCYb) perovskites and strontium doped and $La_{0.995}Sr_{0.005}NbO_{4+\delta}$ (LNb) monazite were synthesized by spray-pyrolysis at the Norwegian University of Science and Technology (NTNU), according to a proprietary method, using water-based solutions.[8] The precursor materials were calcined in air at 1000 °C for 48 h for BZY, 800 °C for 10:00 h for LNb, and 1000 °C for 6:00 h for SCYb in order to obtain fully crystallized powders.

For the preparation of Ni-based composite anodes, NiO powder was purchased at GFS Chemicals. Tape-casting was applied for the production of SCYb porous supports and LNb/NiO anodes (20.5 wt.%/22.5 wt.%). The powders were firstly mixed in an azeotropic mixture of methylethylketone and ethanol, using a planetary mill with zirconia balls and mortar. Butvar B-98 commercial binder (7 wt.%, Monsanto, US) and two plasticizers, such as polyethyleneglycol (3 wt.%) and dibutylphtalate (3 wt.%) were then added to provide adequate strength and plasticity to the green tapes. For tailoring anodes porosity, corn starch filler (4 wt.%) was added in the slurries.

The slurry was cast onto a Mylar™ film and left drying overnight at room temperature in a closed box. Several dried tapes of 10 cm × 10 cm dimensions were laminated at 45 °C with a pressure of 5 tons applied for 30 s. Green laminates of 20 mm in diameter were heated up to 550 °C at a heating rate of 10 °C h^{-1} and subsequently held for 10 h to burnout organic compounds. A further annealing step at 1000 °C for 2 h was conducted to achieve sufficient strength.

Stable ceramic colloidal suspensions were prepared by dispersing SCYb, BZY or LNb powders (13 wt.%) in a mixture of methylethylketone and terpineol (60/40 vol.%). Butvar B-98 binder (0.03 wt.%) was also added. The suspensions were homogenised for 2 h in a planetary mill at 360 rpm. Their viscosity ranges from 10 to 25 mPa s, depending on the ceramic powder used. The suspensions were then spin-coated once onto the porous layers with a spinning speed of 2000 rpm for 30 s. The half-cells (electrolytes + anodes) and membranes were sintered in air at 1350 °C for 2 h, with a heating rate of 100 °C/h. The sintered half-cells were thereafter screen-printed using a commercial Pt ink and subsequently annealed at 1000 °C for 2 h. The compositions of both slurries and suspensions are reported in Table 1.

Table 1
Composition of slurries and suspensions

	Powders	Dispersant	Binder + plasticizer
SCYb support	33	0.02	15
BZY anode	43	0.01	6
LNb anode	43	0.01	6
SCYb membrane	19, 50	0.02	0.03
BZY electrolyte	19	0.02	0.03
LNb electrolyte	13, 19	0.02	0.03

Values are indicated in weight percentage calculated from the total weight of the solutions.

2.2. Characterization of powders and films

XRD analysis was carried out with a Siemens D710 diffractometer. The ceramic particles size distribution in the fresh slurries and in the suspensions was evaluated using a Mastersizer 2000 particle size analyzer. For scanning electron microscopy (SEM) observations, both membranes and fuel cells were embedded in an epoxy resin. Cross-sections of embedded samples were carefully polished down to 1 μm using SiC grinding papers followed by diamond suspension. The samples were examined with a JEOL JSM-5900LV SEM using back scatter electron detector. The gas tightness of the dense layers was examined at room temperature using a measurement cell with a rubber gasket sealing. Helium leakage was investigated by concentration cell measurements using 60 ml/min of helium as feed gas and 50 ml/min of argon ($pO_2 \approx 10^{-3}$) as permeate sweep gas. The concentration of helium in the permeate gas after passing through the membrane was determined by gas chromatography.

3. Results and discussion

BZY, LNb and SCYb spray-pyrolysed powders are fairly agglomerated and exhibit a narrow particle size distribution with a mean size of about 150 nm (Fig. 1).

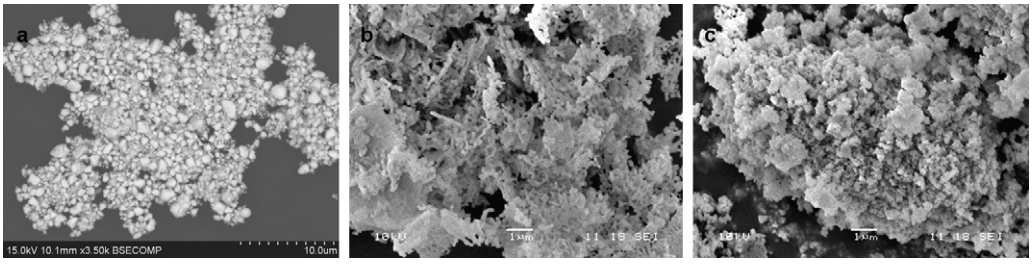

Fig. 1. SEM micrographs of (a) SCYb, (b) LNb and (c) BZY spray-pyrolysed powders.

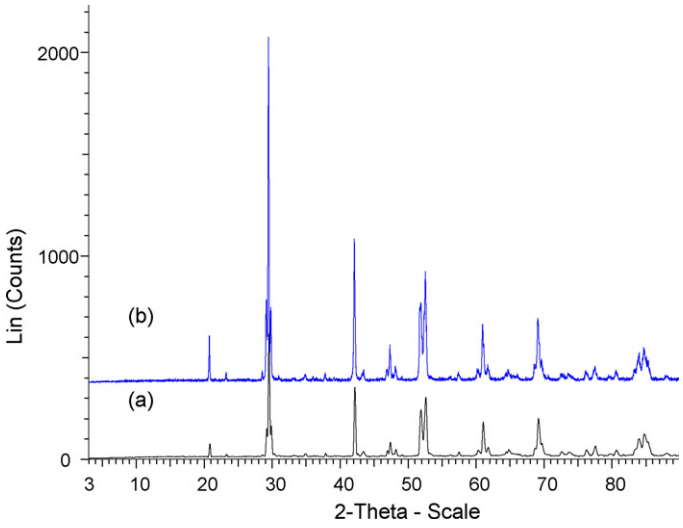

Fig. 2. XRD pattern of SCYb powder (a) and membrane (b).

XRD patterns taken for all spray-pyrolysed powders are shown in Figs. 2–4. All patterns were indexed with a single phase structure of the corresponding perovskite for SCYb (Fig. 2a) and BZY (Fig. 3a) and of the monazite phase for LNb (Fig. 4a), in agreement with literature data.[4,5] The crystallographic density was extracted from Rietveld refinement of XRD patterns and is 5.81 g cm^{-3} for SCYb, 5.90 g cm^{-3} for LNb and 6.21 g cm^{-3} for BZY.

The particles size distribution of powders dispersed in the slurries used for tape-casting and in the suspensions used for spin-coating is shown in Fig. 5a–c. For all samples, the distribution is characterized by two peaks centred at ~150 nm and ~1.5 μm. The former contribution is attributed to the presence of primary particles, while the latter indicates the presence of agglomerates in the suspensions, in agreement with SEM observations. These solutions were stable for several days and were thus used for tape-casting and spin-coating.

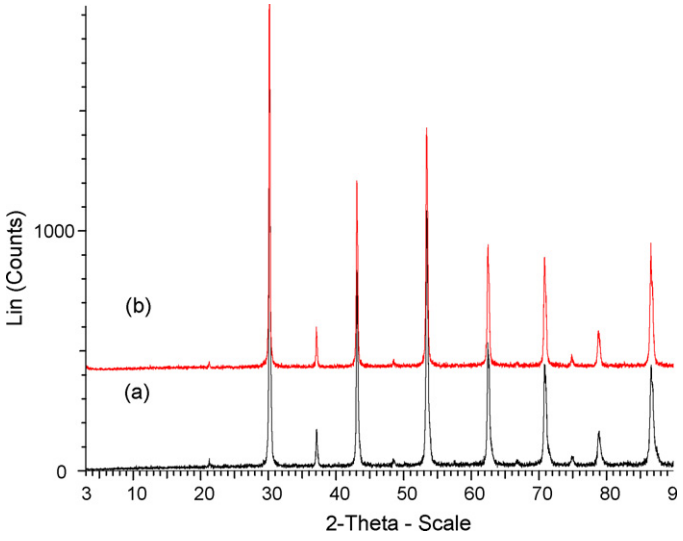

Fig. 3. XRD pattern of BZY powder (a) and sintered electrolyte (b).

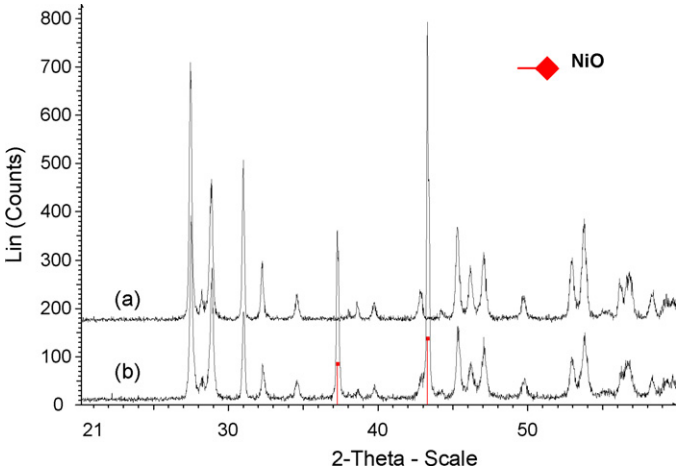

Fig. 4. XRD pattern of LNb powder (a) and sintered electrolyte (b).

In this work, three types of cells were investigated. Novel PCFCs consisting of LNb electrolyte coated onto LNb–NiO anode were prepared to take advantage of the high mechanical and chemical stability of LNb material. For comparison, cells of BZY electrolyte coated onto BZY/NiO anode were also investigated. Further, original 'mixed' cells integrating BZY electrolyte coated onto LNb/NiO anodes were prepared to prevent potential degradation of BZY material in CO_2 atmosphere. SEM micrographs of BZY–LNb/NiO, BZY–BZY/NiO and LNb–LNb/NiO cells are shown in Figs. 6 and 7. SCYb membranes are shown in Fig. 8.

All samples remained flat after sintering. SCYb membranes and LNb electrolytes coated onto LNb/NiO anodes were fully dense. The thickness of the functional layer increases with increasing ceramic solid loading in suspension and is ranging from 4 to 25 μm for SCYb membranes (Fig. 8), and from 9 to 26 μm for LNb electrolytes (Fig. 7). The dense layers exhibit homogeneous composition and show good adhesion to the underlying porous supports. The gas tightness of the functional layers was confirmed by checking potential He leakage at room temperature. No leakage was detected by gas chromatography indicating that both LNb electrolytes and SCYb membranes were free of transversal crack or connected pores. XRD analysis performed on both sides of samples confirmed that no change in material composition and structure occurred during sintering at 1350 °C (Figs. 2b and 4b).

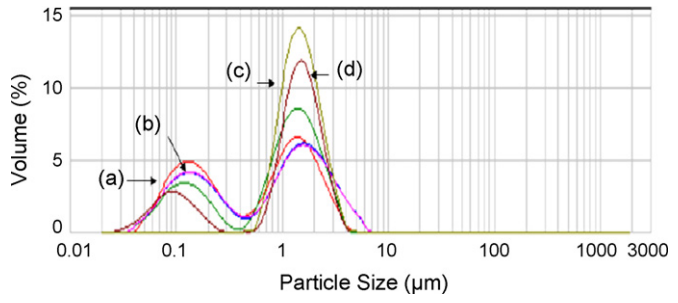

Fig. 5. Particle size distributions of (a) LNb in suspension; (b) LNb in slurry; (c) BZY in suspension; (c) SCYb in suspension.

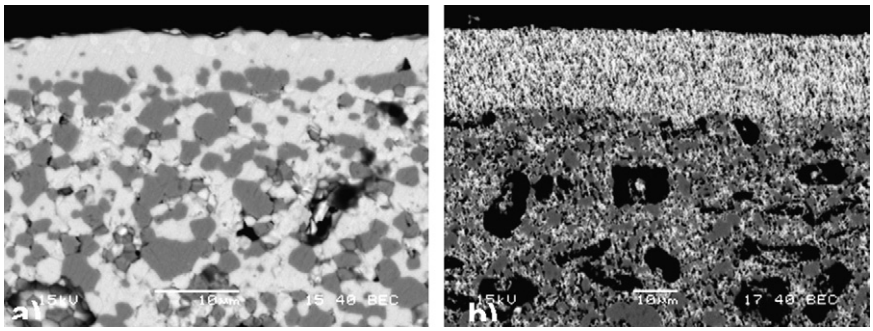

Fig. 6. SEM micrographs of cells with BZY electrolytes sintered at 1350 °C for 2 h and coated onto (a) LNb/NiO anode and (b) BZY/NiO anode. The solid loading in suspension is 19 wt.%.

SEM analyses reveal drastic changes in BZY electrolyte microstructure depending on the anode support (Fig. 6). The "mixed cell" exhibited a fully dense and leak-free BZY electrolyte with a thickness of 4 μm after sintering at 1350 °C (Fig. 6a). XRD pattern of BZY electrolyte (Fig. 3b) indicates that the electrolyte is single-phase and no interfacial reaction between BZY and LNb/NiO anode is observed. There was no visible delamination between the electrolyte and the anode layers after sintering, as expected since LNb and BZY have close thermal expansion coefficient of $\sim 8 \times 10^{-6}$ and $\sim 7 \times 10^{-6}\,K^{-1}$, respectively. In contrast, BZY electrolyte coated onto BZY/NiO anode remains highly porous (Fig. 6b). In order to explain the differences encountered while using either BZY/NiO or LNb/NiO anodes, the sintering shrinkage of half-cells was calculated from the measurement of anodes geometrical dimensions. The results are depicted in Fig. 9.

LNb/NiO anode-supported cells shrunk about 36% after sintering at 1350 °C, seemingly independently of the electrolyte materials. It should be emphasized that this shrinkage is similar to that observed on un-coated anodes sintered at the same temperature. In contrast, BZY/NiO anode-supported cells only shrunk ~10% at 1350 °C. The cells were thus annealed at higher temperature in an attempt to achieve higher shrinkage. Nevertheless, increasing sintering temperature up to 1650 °C only led to a shrinkage of 30%, while the electrolyte remained porous. One may therefore presume that the larger contraction of LNb/NiO anode during sintering imposes larger shrinkage to the BZY electrolyte layer, which promotes faster sintering kinetics. This sintering temperature is low compared to data published in the literature, which usually referred to temperatures above 1500 °C for BZY material.[12–13]

The coating of the Pt cathode and its subsequent annealing did not affect the flatness of the fuel cells. Samples remained

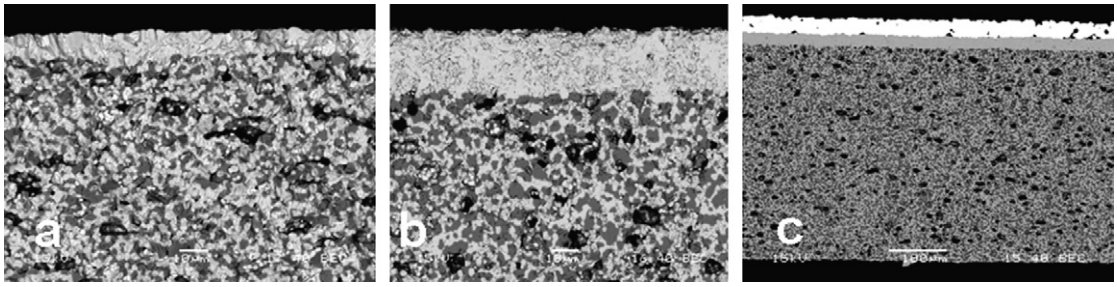

Fig. 7. SEM micrographs of fuel cells with LNb electrolyte coated onto LNb/NiO anode sintered at 1350 °C for 2 h. The solid loading in suspension is (a) 13 wt.% and (b) 19 wt.% Pt cathode is screen-printed (c).

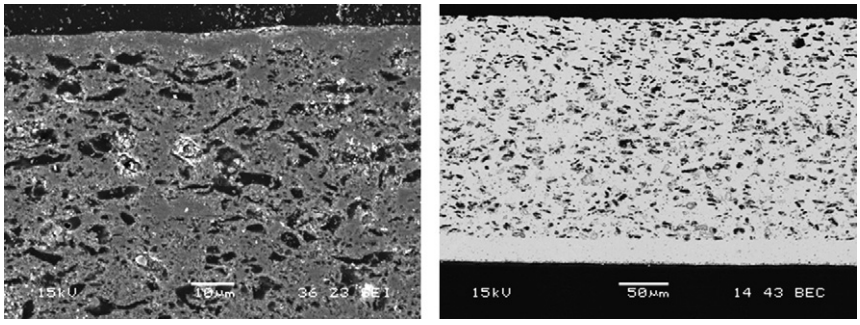

Fig. 8. SEM micrographs of SCYb membrane sintered at 1350 °C for 2 h. The solid loading in suspension is 19 wt.% (on the left) and 50 wt.% (on the right).

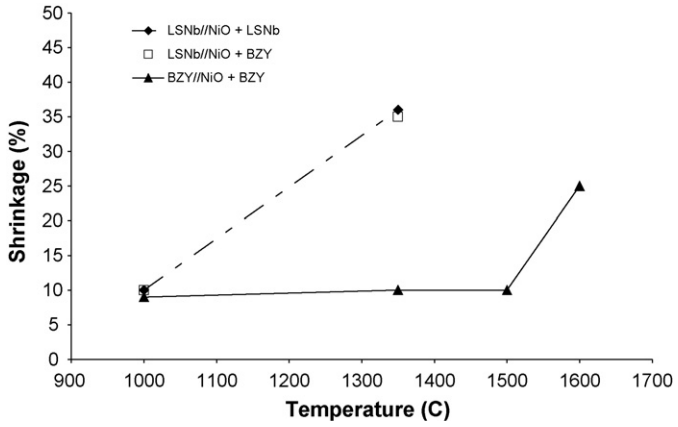

Fig. 9. Evolution of samples radial shrinkage as a function of the annealing temperature.

crack-free and neither shrinkage nor phase reaction between the different layers was detected.

4. Conclusion

We have developed a time- and cost-effective process for the preparation of dense ceramics films of protonic conductors based on ceramic powders produced by spray-pyrolysis. SCYb asymmetric membranes and new PCFC devices integrating state-of-the-art BZY or novel LNb proton conducting thin film electrolytes with a thickness ranging from 4 to 26 μm, were produced by a versatile process combining reliable techniques, which make it potentially cost-effective and easy to up-scale. The new architectures were based on semi-monolithic cells with LNb material present in all functional layers to take advantages of its chemical and mechanical stability and inherent materials integration. Mixed cells combining LNb-based anode and BZY electrolyte were also successfully produced in order to benefit of the high grain interior conductivity of BZY electrolyte material, while avoiding issue regarding its stability as anode-based material. A dramatic decrease in the sintering temperature of BZY and LNb electrolytes was demonstrated in this work, as both electrolytes were fully dense after annealing in air at 1350 °C without pressure or sintering aids assistance. This alleviated sintering process enables controlling materials composition and microstructure, and avoids interfacial reaction between the functional layers.

Acknowledgements

The work was supported by The Research Council of Norway (NANOMAT), Grant no. 158517/431 (Functional Oxides for Energy Technology). Thanks are due to PhD-students Tommy Mokkelbost* and Paul Inge Dahl* and Post doc. Hilde L. Lein, all at NTNU, for providing SEM pictures and giving useful guidelines concerning sintering. *Permanent address is Sintef Materials and Chemistry.

References

1. Abrutis, A., Teiserskis, A., Garcia, G., Kubilius, V., Saltyte, Z., Salciunas, Z. *et al.*, *Journal of Membrane Science*, 2004, **240**, 113.
2. Schneller, T. and Schober, T., *Solid State Ionics*, 2003, **164**, 131.
3. Hamakawa, S., Li, L., Li, A. and Iglesia, E., *Solid State Ionics*, 2002, **48**, 71.
4. Xia, C., Ward, T. L., Atanasova, P. and Schwartz, R. W., *Journal of Materials Research*, 1998, **13**, 173.
5. Meng, G. Y., song, H. Z., Wang, H. B., Xia, C. R. and Peng, D. K., *Thin Solid Films*, 2002, **409**, 105.
6. Itoh, H., Asano, H., Fukuroi, K., Nagata, M. and Iwahara, H., *Journal of American Ceramic Society*, 1997, **80**, 1359.
7. Zhu, Q. and Fan, B., *Solid State Ionics*, 2005, **176**, 889.
8. Norby, T., Haugsrud, R., Strøm, R.A., Grande, T., Wiik, K. and Einarsrud, M.-A., *Patent application*, 2005.
9. Haugsrud, R., Fjeld, H., Haug, K. R. and Norby, T., *Journal of The Electrochemical Society*, 2007, 77.
10. Kreuer, K. D., Adams, S., Münch, W., Fuchs, A., Klock, U. and Maier, J., *Solid State Ionics*, 2001, **145**, 295.
11. Aksenova, T. I., Khromushin, I. V., Zhotabaev, K. D., Bukenov, A. K., Berdauletov, Z. V. and Medvedeva, *Solid State Ionics*, 2003, **162-16**, 31.
12. Snijkers, F. M. M., Buekenhoudt, A., Cooymans, J. and Luyten, J. J., *Scripta Materialia*, 2004, **50**, 655.
13. Schober, T. and Bohn, H. G., *Solid State Ionics*, 2000, **127**, 351.